Infectious Disease Modelling 9 (2024) 1095–1116

Contents lists available at ScienceDirect

Infectious Disease Modelling

journal homepage: www.keaipublishing.com/idm

Modeling and investigating malaria P. Falciparum and P. Vivax infections: Application to Djibouti data

Yahyeh Souleiman [a, *], Liban Ismail [a], Raluca Eftimie [b]

[a] Centre de Recherche en Mathématiques et Numérique (CRMN), University of the Djibouti, Campus Balbala, Djibouti
[b] Laboratoire Mathématiques de Besançon (LMB), University of Bourgogne Franche-Comté, Besançon, France

ARTICLE INFO

Article history:
Received 28 March 2024
Received in revised form 3 June 2024
Accepted 14 June 2024
Available online 16 June 2024
Handling Editor: Dr Daihai He

Keywords:
Falciparum and vivax models
Reproduction number
Stability analysis
Sensitivity analysis
FAST method
LHS method
Djibouti data

ABSTRACT

Malaria is an infectious and communicable disease, caused by one or more species of Plasmodium parasites. There are five species of parasites responsible for malaria in humans, of which two, Plasmodium Falciparum and Plasmodium Vivax, are the most dangerous. In Djibouti, the two species of Plasmodium are present in different proportions in the infected population: 77% of P. Falciparum and 33% of P. Vivax. In this study we present a new mathematical model describing the temporal dynamics of Plasmodium Falciparum and Plasmodium Vivax co-infection. We focus briefly on the well posedness of this model and on the calculation of the basic reproductive numbers for the infections with each Plasmodium species that help us understand the long-term dynamics of this model (i.e., existence and stability of various eqiuilibria). Then we use computational approaches to: (a) identify model parameters using real data on malaria infections in Djibouti; (b) illustrate the influence of different estimated parameters on the basic reproduction numbers; (c) perform global sensitivity and uncertainty analysis for the impact of various model parameters on the transient dynamics of infectious mosquitoes and infected humans, for infections with each of the Plasmodium species. The originality of this research stems from employing the FAST method and the LHS method to identify the key factors influencing the progression of the disease within the population of Djibouti. In addition, sensitivity analysis identified the most influential parameter for Falciparium and Vivax reproduction rates. Finally, the uncertainty analysis enabled us to understand the variability of certain parameters on the infected compartments.

1. Introduction

Malaria is one of the deadliest infectious diseases that has claimed million of lives around the world. In 2022, the World Health Organization (WHO) (World Health Organization, 2022) estimated that there would be 249 million cases of malaria and 608 000 malaria-related deaths in 85 countries. The evolutionary potential of parasites and vectors, the rise and fall of human immunity, changes in the behavior of human and vector populations, and the interactions among the many heterogeneous subpopulations complicate the development of programs and policies optimal for the control of infectious diseases. Malaria is an infectious disease caused by the Plasmodium parasite, transmitted by the bites of an infected female

* Corresponding author.
E-mail address: yahyeh_souleiman_isman@univ.edu.dj (Y. Souleiman).
Peer review under responsibility of KeAi Communications Co., Ltd.

https://doi.org/10.1016/j.idm.2024.06.003

Anopheles mosquito (Ogunmiloro, 2019; Somma et al., 2017). According to the World Health Organization (WHO) (Hay et al., 2005; World Health Organization, 2022), the estimated number of deaths from malaria is 580 000, with Africa recording 95% of fatalities. The different parasite species responsible for malaria include P. falciparum, P. vivax, P. malariae, P. knowlesi, P. ovale wallikeri, P. ovale curtisi (Garrido-Cardenas et al., 2019; Hay et al., 2005; Loy et al., 2017). Moreover, according to the World Health Organization (WHO), children under five account for 80% of malaria deaths in the African region. In sub-Saharan Africa (Rodriguez-Morales, 2008), it is the second leading cause of death after HIV/AIDS. Malaria is caused by parasites of the genus Plasmodium transmitted to humans through the bites of infected female Anopheles mosquitoes, called "malaria vectors". There are five species of parasites that cause malaria in humans, two of which, Plasmodium falciparum and Plasmodium vivax, are the most dangerous (Mueller et al., 2009). In 2018, P. falciparum accounted for 99.7% of estimated malaria cases in the WHO African Region, 50% of cases in the South-East Asia Region, 71% of cases in the Eastern Mediterranean region and 65% of cases in the Western Pacific region (Nnamonu et al., 2020; Sankineni et al., 2023).

In Djibouti, the two species of malaria parasites are present in different proportions (Khaireh et al., 2013; Moussa et al., 2023): 77% of P. falciparum and 33% of P. vivax. The mosquito species Anopheles Arabiensis and Anopheles Stephensi are two major vectors of malaria in the country. These 2 vectors are at the root of the epidemics that have hit the country since 2013. The country recorded an increase in malaria cases in 2015. From January 2019 to December 2019, a total of 49402 malaria cases out of the 220 381 examined (a positivity rate of 22.42% and an incidence of 49.76 cases per 1000 inhabitants) were affected by malaria in the population. More recently, the annual number of reported malaria cases in 2020 is 73.535. In the same period the first case of Covid19 was confirmed in March 2020 in Djibouti and the article (Souleiman et al., 2021) was published on the dynamics of the disease. The complexity of the parasite life cycle, its high genetic variability and the many mechanisms it can develop to evade the host immune response, make it very difficult to find a vaccine to suppress human malaria (Flores-Alanis et al., 2017; Tuju et al., 2017). Additionally, the biology of P. vivax, as opposed to P. falciparum, makes its control and elimination more difficult. In (White et al., 2018) the authors study the duration of re-infections, recrudescences and relapses of P. vivax and P. falciparum. Other reasons are related to the presence of hypnozoites (latent liver forms), which lead to multiple relapses and low parasite densities, which makes diagnosis difficult and delays treatment (Olliaro et al., 2016). On the other hand, there are no suitable experimental models for the analysis of a hypothetical vaccine. Despite this, finding a vaccine to eradicate malaria caused by P. vivax has become a fundamental goal for WHO and scientific communities around the world.

While there are numerous mathematical modelling studies that investigate malaria infections (see the review paper (Mandal et al., 2011) and the references therein) most of them focus on infections with single Plasmodium species. There are also a few studies that focused on the co-infections between malaria and other viruses/bacteria: in (Ray et al., 2020; Sardar et al., 2020) the authors investigate malaria-COVID-19 co-infections, in (Mukandavire et al., 2009a; Seidu et al., 2015; Shah & Gupta, 2014) the authors investigate malaria-HIV co-infections, in (Long et al., 2008; Porco et al., 2001) the focus is on malaria-tuberculosis co-infections, in (Okosun & Makinde, 2014) the focus on malaria-cholera co-infection, while in (Mensah et al., 2018) the focus is on malaria-zika co-infection. Even fewer studies focused on triple co-infections between malaria, dengue and typhoid infections (Deshkar et al., 2015; Oluwafemi et al., 2020; Suresh et al., 2013). Nevertheless, all these studies focus on a single malaria species. Yet, in many geographical areas there are co-infections with multiple Plasmodium species, and their particular dynamics impacts the persistence of the infections and the success of the treatment. Among the very few mathematical models derived to investigate co-infections with multiple Plasmodium species we remark two studies: (i) the study in (Mahato et al., 2015) focused on Indian data that showed slightly more infections with P. Vivax compared to P. Falciparum in late 1990's and almost the same number of infections with P. Vivax and P. Falciparum in 2010; and (ii) the theoretical study in (Workie & Koya, 2022) focused on modelling a triple infection with typhoid fever, P. Vivax and P. Falciparum, but which did not focus on specific data. Nevertheless, investigating the dynamics of P. Vivax and P. Falciparum in the context of data for specific geographical regions is extremely important for the understanding of the transmission of the infections with these two species, and the short-term/medium-term evolution of their dynamics.

In this study we propose a mathematical model for the dynamics of the P. Vivax and P. Falciparum the infections, as informed by the specific Djibouti data that we use to estimate our model parameters. Due to the paucity of data in our possession, in this article we will assume that there will be no interaction between the two malaria vectors (Falciparium and Vivax). These data will also be illustrated by sensitivity analyses with Sobol' indices introduced in 1993 in the seminal work (Sobol, 2001). Assuming finite second order moment for the model, the computation of these indices is based on the decomposition of the variance. The main objective of this work is to apply the Fourier Amplitude Sensitivity Test (FAST) method and the Latin Hypercube Sampling (LHS) method (Marino et al., 2008; Massard et al., 2022) to identify the factor that most influences the evolution of the disease in the population. We will also use the Monte Carlo method to compare results on sensitivity analysis. This approach allows us to: (i) understand the transmission of malaria in Djibouti; (ii) compare our results with data-informed modelling results in other geographical regions in the world where the two Plasmodium species are present, so we can draw conclusions about the evolution of these infections in response to the specific characteristics of these different geographical regions.

The remainder of the paper is organized as follows: in section 2, we present the mathematical model describing infection dynamics, as well as the positivity and boundedness of the solutions to verify that the model is well-posed. In section 3, to better understand the complete model with the infection of the two pathogens, we start by first studying the two sub-models characterised by single infections: the sub-model with P. Falciparum infection and the sub-model with P. Vivax infection, before returning to the full model. The details of this section are found in the appendix, where we calculate the basic reproduction number for the infection dynamics of Plasmodium Falciparum and Plasmodium Vivax. Then, we present the existence of disease-free and endemic equilibrium points in the models and use a nonlinear stability analysis method to prove

the local stabilities of these equilibrium. And finally, in section 4, we estimate the essential parameters and conduct a global sensitivity analysis using both the FAST and LHS methods to identify the most influential factors on the reproduction base rates.

2. Model formulation

The total human N_h population is divided into four classes. Indeed, the susceptible individuals S_h, the individuals infected by plasmodium falciparum I_{fh} and by plasmodium vivax I_{vh}, the recovered individuals R_h. Thus, the total human population is

$$N_h(t) = S_h(t) + I_h(t) + R_h(t),$$

with, $I_h(t) = I_{fh}(t) + I_{vh}(t)$. The total mosquito N_m population is divided into three classes, the susceptible classes S_m and the two infective classes by plasmodiums falciparum I_{fm} and vivax I_{vm}. Thus, at time t, the total population of mosquitoes is

$$N_m(t) = S_m(t) + I_m(t),$$

with, $I_m(t) = I_{fm}(t) + I_{vm}(t)$. In the rest of this section, we present a description of the variables involved, the graph and the system of differential equations describing the model.

Fig. 1 below shows the diagram of the model studied in this paper, where the dotted light-blue arrow represents disease transmission from a falciparum-infected (respectively, vivax-infected) mosquito to a healthy human via the solid light-pink arrow, while the dotted light-pink arrow represents disease transmission from a falciparum-infected (respectively, vivax-infected) human to a healthy mosquito.

The transmission dynamics of malaria are given by the following mathematical model:

$$\begin{cases} \dfrac{dS_h}{dt} = \tau_h + d_h R_h - (\mu_h N_h + \lambda_{fh}\, b\, I_{fm} + \lambda_{vh}\, b\, I_{vm})\dfrac{S_h}{N_h}, \\ \dfrac{dI_{fh}}{dt} = \lambda_{fh}\, b\, I_{fm}\dfrac{S_h}{N_h} - (\mu_h + \mu_{fh} + \alpha_{fh})I_{fh}, \\ \dfrac{dI_{vh}}{dt} = \lambda_{vh}\, b\, I_{vm}\dfrac{S_h}{N_h} - (\mu_h + \mu_{vh} + \alpha_{vh})I_{vh}, \\ \dfrac{dR_h}{dt} = \alpha_{fh}I_{fh} + \alpha_{vh}I_{vh} - (\mu_h + d_h)R_h, \\ \dfrac{dS_m}{dt} = \tau_m - (\mu_m N_h + \lambda_{fm}\, b\, I_{fh} + \lambda_{vm}\, b\, I_{vh})\dfrac{S_m}{N_h}, \\ \dfrac{dI_{fm}}{dt} = \lambda_{fm}\, b\, I_{fh}\dfrac{S_m}{N_h} - \mu_m I_{fm}, \\ \dfrac{dI_{vm}}{dt} = \lambda_{vm}\, b\, I_{f_v}\dfrac{S_m}{N_h} - \mu_m I_{vm}. \end{cases} \tag{1}$$

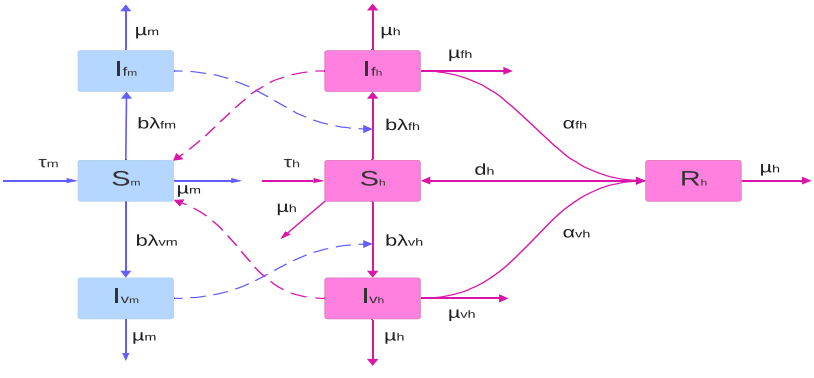

Fig. 1. Schematics model diagram.

Table 1
Model parameters and their descriptions.

Notation	Description
λ_{fm}	Infection P.falciparum transmission probability in mosquitoes
λ_{fh}	Infection P.falciparum transmission probability in humans
λ_{vm}	Infection P.vivax transmission probability in mosquitoes
λ_{vh}	Infection P.vivax transmission probability in humans
μ_{fh}	Death rate due to infection with P.falciparum
μ_{vh}	Death rate due to infection with P.vivax
μ_m	Natural death rate of mosquitoes
μ_h	Natural death rate of humans
α_{fh}	Recovery rate of humans infected by P.falciparum
α_{vh}	Recovery rate of humans infected by P.vivax
τ_h	Constant total recruitment rate of susceptible humans
τ_m	Constant total recruitment rate of susceptible vectors
B	Average biting rate of mosquitoes on humans
d_h	Rate at which recovered individuals become again susceptibles

These are the equations of a dynamic epidemiological model of malaria taking into account both Plasmodium falciparum and Plasmodium vivax, including a return of the cure to the sensitive human compartment, and equations for mosquitoes. Where, S_h represents the number of susceptible individuals to contract malaria, I_{fh} and I_{vh} represent the number of individuals infected with P. falciparum and P. vivax respectively, R_h represent the number of individuals recovered, S_m represents the number of susceptible mosquitoes, I_{fm} and I_{vm} represent the number of mosquitoes infected with P. falciparum and P. vivax respectively, N_h is the total human population size, λ_{fh} and λ_{vh} are the respective transmission rates of P. falciparum and P. vivax from humans to mosquitoes, λ_{fm} and λ_{vm} are the respective transmission rates of P. falciparum and P. vivax from mosquitoes to humans, d_h is the respective recovery rates in humans, μ_h and μ_m are the respective mortality rates of humans, mosquitoes and descriptions of all parameters are given in Table 1 below.

The basic dynamic characteristics of model (1) will now be explored. Since the model monitors human and mosquito populations, all of its associated parameters and state variables are positive for $t \geq 0$. The model assumptions are given in Theorems 1 and 2, and their proofs are presented in Appendix A. For model (1) to be epidemiologically significant, it is important to prove that all its state variables are positive for all times. That is, the solutions of model (1) with positive initial data will remain positive for all $t > 0$.

Theorem 1. *Let the initial data be* $S_h(0) \geq 0$, $S_m(0) \geq 0$, $I_{fh}(0) \geq 0$, $I_{vh}(0) \geq 0$, $I_{fm}(0) \geq 0$, $I_{vm}(0) \geq 0$ *and* $R_h(0) \geq 0$. *We assume that* $R_h(t) \geq 0$ *is positive then the solutions of the model* (1), *with positive initial data, will remain positive, i.e.,* $S_h(t) \geq 0$, $S_m(t) \geq 0$, $I_{fh}(t) \geq 0$, $I_{vh}(t) \geq 0$, $I_{fm}(t) \geq 0$ *and* $I_{vm}(t) \geq 0$ *for all time* $t > 0$.

The above result represents bounding the solution in the theorem.

Theorem 2. *The closed region*

$$\Omega = \left\{ \left(S_h, S_m, I_{fh}, I_{vh}, I_{fm}, I_{vm}, R_h \right) \in \mathbb{R}_+^7 : N_h \leq \frac{\tau_h}{\mu_h}, N_m \leq \frac{\tau_m}{\mu_m} \right\},$$

is positively invariant sets for the system (1).

3. Analysis of the all models

To have a better understanding of the full model with the infection of the two pathogens, we start by investigating first the two sub-models characterised by single infections.The sub-model with the Plasmodium falciparum infection (sub-section 3.1) and the sub-model with the Plasmodium vivax infection (sub-section 3.2). Finally we will return to the analysis of the full model (sub-section 3.3).

3.1. Plasmodium falciparum model

Here, we study the dynamics of the falciparum sub-model only. Taking $I_{vh} = I_{vm} = 0$, we obtain:

$$\begin{cases} \dfrac{dS_h}{dt} = \tau_h + d_h R_h - (\mu_h\ N_h + \lambda_{fh}\ b\ I_{fm})\dfrac{S_h}{N_h}, \\ \dfrac{dI_{fh}}{dt} = \lambda_{fh}\ b\ I_{fm}\dfrac{S_h}{N_h} - (\mu_h + \mu_{fh} + \alpha_{fh})I_{fh}, \\ \dfrac{dR_h}{dt} = \alpha_{fh} I_{fh} - (\mu_h + d_h)R_h, \\ \dfrac{dS_m}{dt} = \tau_m - (\mu_m\ N_h + \lambda_{fm}\ b\ I_{fh})\dfrac{S_m}{N_h}, \\ \dfrac{dI_{fm}}{dt} = \lambda_{fm}\ b\ I_{fh}\dfrac{S_m}{N_h} - \mu_m I_{fm}, \end{cases} \tag{2}$$

The solutions of this sub-model system exist in a space limited by the total human population N_h and mosquito population N_m:

$$\Omega_f = \left\{ \left(S_h, S_m, I_{fh}, I_{fm}, R_h\right) \in \mathbb{R}_+^5 : N_h \leq \frac{\tau_h}{\mu_h}, N_m \leq \frac{\tau_m}{\mu_m} \right\}.$$

As in the previous theorem 2, the closed region Ω_f is a positive invariant set for the system (2).

The basic reproduction number $\mathcal{R}_{0f}$, also called the basic reproduction rate, is an epidemiological metric used to describe the contagiousness or transmissibility of infectious agents. This number is the average number of susceptibles that an infected person will infect at the start of the epidemic. This parameter describing the average number of new infections due to a sick individual, plays a crucial role. Using next generation matrix (Diekmann et al., 2010), the basic reproduction number of (2) can be found. To this end, we start by calculating the disease-free equilibrium (DFE) point for system (2): DFE is $E_{0f} = (\frac{\tau_h}{\mu_h}, 0, 0, \frac{\tau_m}{\mu_m}, 0)$, the reproduction number of the Plasmodium falciparum model (2) is given by the following expression (for details see Appendix B)

$$\mathcal{R}_{0f} = \sqrt{\frac{\lambda_{fm}\lambda_{fh} b^2 \tau_m \mu_h}{\tau_h \mu_m^2 (\mu_h + \mu_{fh} + \alpha_{fh})}}. \tag{3}$$

The following Theorem emphasises the importance of this reproduction number for the existence and stability of the steady states of model (2), that characterize the long-term behaviour of this sub-model. For the proof of this Theorem see Appendix B.

Theorem 3. *The DFE point* (E_{0f}), *which exists for all parameters, is locally asymptotically stable if* $\mathcal{R}_{0f} < 1$. *The endemic equilibrium exists and is unique if conditions* (12) *are satisfied, i.e., if* $R_{0f} > 1$. *In this case the DFE is unstable.*

3.2. Plasmodium vivax model

Here, we study the dynamics of the vivax sub-model only. Taking $I_{fh} = I_{fm} = 0$, we obtain:

$$\begin{cases} \dfrac{dS_h}{dt} = \tau_h + d_h R_h - (\mu_h\ N_h + \lambda_{vh}\ b\ I_{vm})\dfrac{S_h}{N_h}, \\ \dfrac{dI_{vh}}{dt} = \lambda_{vh}\ b\ I_{vm}\dfrac{S_h}{N_h} - (\mu_h + \mu_{vh} + \alpha_{vh})I_{vh}, \\ \dfrac{dR_h}{dt} = \alpha_{vh} I_{vh} - (\mu_h + d_h)R_h, \\ \dfrac{dS_m}{dt} = \tau_m - (\mu_m\ N_h + \lambda_{vm}\ b\ I_{vh})\dfrac{S_m}{N_h}, \\ \dfrac{dI_{vm}}{dt} = \lambda_{vm}\ b\ I_{vh}\dfrac{S_m}{N_h} - \mu_m I_{vm}. \end{cases} \tag{4}$$

The solutions of this sub-model system exist in a space limited by the total human population N_h and mosquito population N_m:

$$\Omega_v = \left\{ (S_h, S_m, I_{vh}, I_{vm}, R_h) \in \mathbb{R}_+^5 : N_h \leq \frac{\tau_h}{\mu_h}, N_m \leq \frac{\tau_m}{\mu_m} \right\}.$$

As in Theorem 2, the closed region Ω_v is a positive invariant set for the system (4).

The basic reproduction number $\mathcal{R}_{0v}$, is also calculated in the same way above. By using the next generation matrix (Diekmann et al., 2010), the basic reproduction of (4) can be found. Thus, the DFE for system (4) is

$$E_{0v} = \left(\frac{\tau_h}{\mu_h}, 0, 0, \frac{\tau_m}{\mu_m}, 0 \right),$$

and the reproduction number is give by (for details see Appendix C):

$$\mathcal{R}_{0v} = \sqrt{\frac{\lambda_{vm}\lambda_{vh} b^2 \tau_m \mu_h}{\tau_h \mu_m^2 (\mu_h + \mu_{vh} + \alpha_{vh})}}. \tag{5}$$

The following Theorem emphasises the importance of this reproduction number for the existence and stability of the steady states of model (4), that characterize the long-term behaviour of this sub-model. For the proof of this Theorem see Appendix C.

Theorem 4. *The point DFE* (E_{0v}), *which exists for all parameters, is locally asymptotically stable if* $\mathcal{R}_{0v} < 1$. *The endemic equilibrium exists and is unique if conditions* (17) *are satisfied, i.e., if* $R_{0V} > 1$. *In this case the DFE is unstable.*

3.3. Analysis of the full model

After analyzing the dynamics of the two sub-models, Plasmodium Falciparum and Plasmodium Vivax, we now turn our attention to the complete infection model. The basic reproductive number $\mathcal{R}_0$, of an epidemiological model is defined as the average number of secondary cases produced by one infectious individual in an otherwise fully susceptible population where no control measures are implemented. An important objective of any infectious disease control program is to implement control measures effectively to reduce the reproductive number below one. The isolation reproductive numbers in a multi-parasite model, such as this two-parasite malaria model, refer to the basic reproductive numbers for the model when only one parasite species is present at a time. These values are essential for understanding the transmission potential of each parasite species individually within the context of the overall infection model. By analyzing the isolation reproductive numbers, we can gain insights into the dynamics of each parasite species and tailor control strategies accordingly.

Using the next generation operator approach (Diekmann et al., 2010), we find that the control reproductive number $\mathcal{R}_0$ for the malaria model (1) is given by $\mathcal{R}_0 = \max\left(\mathcal{R}_{0f}; \mathcal{R}_{0v}\right)$, where $\mathcal{R}_{0f}$ is the reproductive number for P. falciparum, and $\mathcal{R}_{0v}$ is the reproductive number for P. vivax. These reproductive numbers for P. falciparum and P. vivax are described by the expression (3) and (5) respectively.

Theorem 5. *The DFE for the full model* (1) *is locally asymptotically stable if* $\mathcal{R}_0 < 1$, *otherwise it is unstable.*

The proof of this theorem 5 is based on Theorems 3 and 4 and can be found in Appendix D.

4. Numerical results

This section is devoted to the numerical simulation of the model. As a result, we begin by estimating the parameters, before returning to the sensitivity analysis on the number of basic reproductions. We conclude with a global sensitivity analysis on the infections compartments.

4.1. Parameter estimation

Numerical estimation is an approach to approximating the value of a mathematical quantity using mathematical algorithms and tools. Here, we study numerically the behavior of the systems (2) and (4) using some of the parameter values compatible with malaria in the article (Agusto & Tchuenche, 2013). This method fits a nonlinear model to data on Falciparum and Vivax infections and deaths in Djibouti. The process involves importing cumulative infection and death data, calculating day indices and daily increases, and refining the model through 100 iterations using the "nlinfit" function. Daily increases in infections and deaths are plotted, adjusted, and compared. Numerical estimation is used to approximate mathematical quantities, taking into account estimation errors due to algorithm and data limitations. The parameter set must be identifiable for accurate estimation, involving sensitivity analysis and identifiability analysis to determine which parameters can be estimated based on available observations.

Now, to support the analytically obtained results in the previous section and to get abetter understanding of the behavior of system (1), we perform some numerical simulations. As a result, we are going to compare on the same graph the results of the values of some parameters obtained during the data collection for the case of malaria from January 1, 2022 to April 30, 2022 in Djibouti with those extrapolated. Therefore, it is necessary to partially validate the accuracy of the obtained data. First, we estimate the parameters by sub-model to better identify the structures of the data according to the two vectors Falciparum and Vivax.

Figs. 2 and 3 represent the cumulative cases, infected cases, and deaths from Falciparum which are then interpolated by the deterministic Falciparum sub-model to estimate the most influential parameters such as λ_{fh}, λ_{fm}, α_{fh} and μ_{fh}, in Table 2.

With these estimated parameters in Table 2, we can now simulate the Falciparium sub-model and we obtain Fig. 4 which represents the evolution of the human and mosquito model. This figure show that the disease persists in the population until 20th days. A relatively larger decrease in the infected population as the number of infected mosquitoes decreases. Importantly, the figure shows that the infected populations can be completely controlled for a low rate of mosquito bites on humans. Thus, one can say that the disease can be totally controlled by enhancing the use of disinfectants against the mosquito. For this parametric setup in Table 2, we obtain the value of basic reproduction number as $\mathcal{R}_{0f} = 3.3692 > 1$.

As in the case of the previous figures, Figs. 5 and 6 represent the cumulative cases, infected cases, and deaths from Vivax which are then interpolated by the Vivax sub-model to estimate the most influential parameters such as λ_{vh}, λ_{vm}, α_{vh} and μ_{vh} in Table 3.

Fig. 7 show that the disease persists in the population until 15th days like the case in Fig. 4 but with a smaller peak, when the number of infected mosquitoes begins to decline. There is also a discrepancy in the number of people infected with Plasmodium Falciparum and Plasmodium vivax, respectively, on the death case. This discrepancy shows that Falciparum is more infectious than Vivax. With the parameters in Table 3, we also get the value of the basic reproduction number as $\mathcal{R}_{0v} = 2.6185 > 1$. This gives us the reproduction number of the full model $\mathcal{R}_0 = \max(\mathcal{R}_{0f}; \mathcal{R}_{0v}) = 3.3692 > 1$.

Figs. 8 and 9 show that the importance of average mosquito biting rate on humans to reduce the evolution of the epidemic by infected individuals plays a major role in the control or elimination of the disease. Moreover, we observe that for $b = 0.25$ it gives $\mathcal{R}_0 = \max(\mathcal{R}_{0f}; \mathcal{R}_{0v}) = \max(3.3692; 2.6185) = 3.3692 > 1$, the disease persists inversely for $b = 0.048$ it gives $\mathcal{R}_0 = \max(\mathcal{R}_{0f}; \mathcal{R}_{0v}) = \max(0.647; 0.5027) = 0.637 < 1$, the infection disappears from the community. Finally, we see the impact of this variation for individuals infected by Plasmodium Falciparum and Plasmodium vivax. However, the number of infected individuals decreases with increasing mosquito mortality rates, respectively.

4.2. Sensitivity analysis for the basic reproduction rate

The purpose of sensitivity analysis is to investigate the influence of each input parameter and their possible interactions on the output measures. Sensitivity analysis can be separated into two main methods: local analysis based on a local perturbation around an average value and global analysis that considers input parameters as random variables and decomposes the output variance into several components. Global sensitivity analysis (Homma & Saltelli, 1996; Ismail et al., 2023; Saltelli, 2002; M Sobol, 1993) is a technique that assesses the overall changes in a model's results for larger changes in key model variables. Since the knowledge on the model parameters is incomplete, we now perform a global sensitivity analysis of the different compartments, where we vary all parameters at the same time. For this purpose, we consider the classical Monte Carlo (MC) approach and the Fourier Amplitude Sensitivity Test (FAST) method (Cukier et al., 1973, 1975, 1978). The Fourier Amplitude Sensitivity Test (FAST) is a sensitivity analysis method that uses statistical analysis techniques to assess the uncertainty of the model results. This method was developed by Cukier (Cukier et al., 1973, 1975, 1978) as well as Schaibly and Shuler (Schaibly & Shuler, 1973). It focuses on the first and second moment of the distribution of each key model variable to determine the uncertainty of the model results.

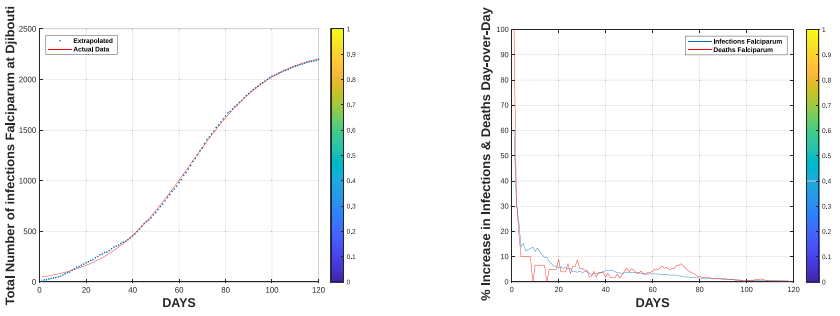

Fig. 2. Approximation on the accumulation of real data of infected cases and the percentage of the ratio between daily infections and daily deaths due to Falciparium Plasmodium in Djibouti.

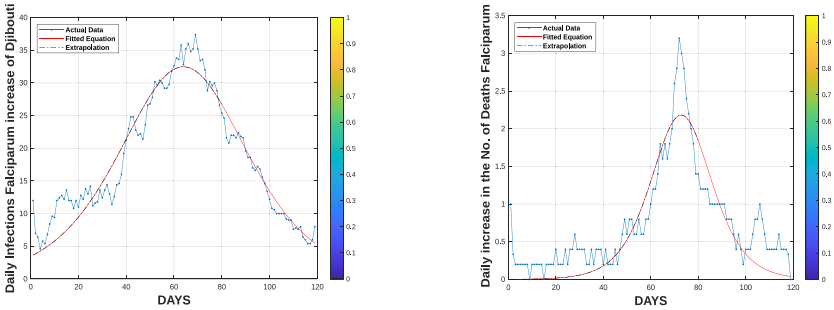

Fig. 3. Approximation of the daily evolution of the real data of infections and deaths due to Falciparum Plasmodium in Djibouti.

Table 2
Parameter estimation for the falciparum model.

Parameter	Value	Reference
τ_h	0.05/day	Mukandavire et al. (2009b)
d_h	0.97202/day	Estimated
τ_m	1000/day	Mushayabasa et al. (2014)
μ_{fh}	0.0405/day	Estimated
μ_h	0.00004/day	Jones et al. (2015)
λ_{fh}	2.4029/day	Estimated
μ_m	0.1429/day	Mukandavire et al. (2009b)
λ_{fm}	0.9391/day	Estimated
B	0.25/day	Mukandavire et al. (2009b)
α_{fh}	0.4462/day	Estimated

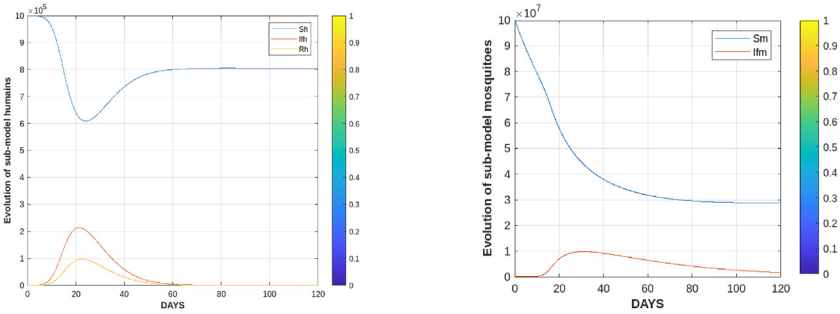

Fig. 4. Evolution humans and mosquitoes of sub-model Falciparum with the estimated parameters $\lambda_{fh} = 2.4029$, $\alpha_{fh} = 0.4462$, $\lambda_{fm} = 0.9391$ and $\mathcal{R}_{0f} = 3.3692$.

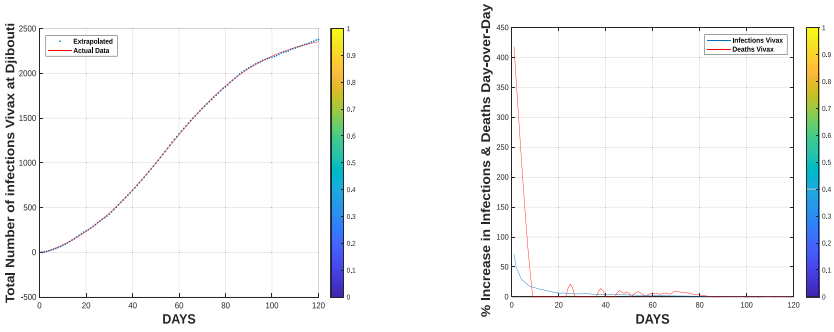

Fig. 5. Approximation on the accumulation of real data of infected cases and the percentage of the ratio between daily infections and daily deaths due to Vivax Plasmodium in Djibouti.

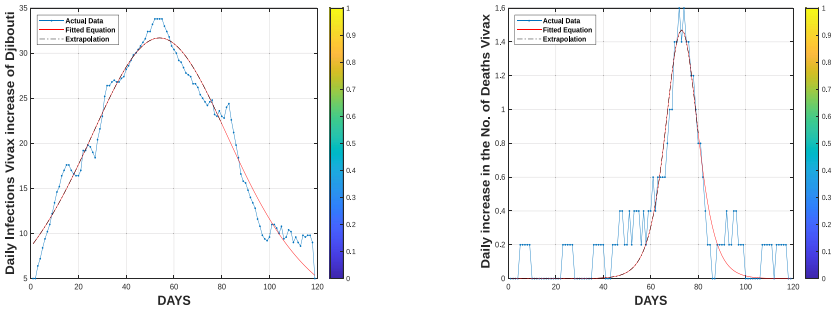

Fig. 6. Approximation of the daily evolution of the real data of infections and deaths due to Vivax Plasmodium in Djibouti.

The fitting method involves the application of sampling and sensitivity analysis techniques, including Saltelli (Saltelli, 2002), FAST (Fourier Amplitude Sensitivity Test) and Latin Hypercube Sampling, to assess the impact of input variables on the basic reproduction rates $\mathcal{R}_{0f}$ of Plasmodium falciparum and $\mathcal{R}_{0v}$ Plasmodium vivax infections.

The objective of the MC and FAST methods is to determine which key model variables have the greatest impact on the model results. We consider the output model defined by (3) and (5),

$$\mathcal{R}_{0f}(\lambda_{fh}, \lambda_{fm}, \alpha_{fh}, \mu_{fh}) = \sqrt{\frac{\lambda_{fm}\lambda_{fh} b^2 \tau_m \mu_h}{\tau_h \mu_m^2 (\mu_h + \mu_{fh} + \alpha_{fh})}},$$

and

$$\mathcal{R}_{0v}(\lambda_{vh}, \lambda_{vm}, \alpha_{vh}, \mu_{vh}) = \sqrt{\frac{\lambda_{vm}\lambda_{vh} b^2 \tau_m \mu_h}{\tau_h \mu_m^2 (\mu_h + \mu_{vh} + \alpha_{vh})}}.$$

We now study the impact on $\mathcal{R}_{0f}$ and $\mathcal{R}_{0v}$ when we vary uniformly the parameters.

We consider that the parameters (λ_{fh}, λ_{fm}, λ_{vh}, λ_{vm}, α_{fh}, α_{vh}) are random and follow the uniform law on the following respective intervals $\lambda_{fh} \in [2.35; 2.45]$, $\lambda_{fm} \in [0.88; 0.98]$, $\lambda_{vh} \in [1.90; 2.00]$, $\lambda_{vm} \in [0.56; 0.66]$, $\alpha_{fh} \in [0.39; 0.49]$, $\alpha_{vh} \in [0.36; 0.46]$, $\mu_{fh} \in [0.035; 0.045]$ and $\mu_{vh} \in [0.010; 0.020]$.

From Table 4, we notice that the parameter λ_{fm} which represents the probability of Falciparum transmission in mosquitoes influence at with 20%. The parameter α_{fh} which represents the recovery rate of Falciparum infected humans is the most influential with 76%. From Table 5, we notice that the parameter λ_{vm} which represents the probability of Vivax transmission in mosquitoes influence at with 31%. The parameter α_{fh} which represents the recovery rate of Vivax infected humans is the most influencial at with 64%. In Tables 4 and 5, as the sum of the indices is very close to 1, we can conclude that the combined effects of the interactions between the parameters on the basic reproduction rates ($\mathcal{R}_{0f}$ and $\mathcal{R}_{0v}$) is considered negligible.

In the context of this paper, sensitivity analysis is used to assess the impact of uncertainty in the parameters (λ_{fh}, λ_{fm}, λ_{vh}, λ_{vm}, α_{fh}, α_{vh}) on the respective base reproduction rates ($\mathcal{R}_{0f}, \mathcal{R}_{0v}$) of sub-models (2) and (4). We used this analysis to assess the robustness of the model results and to identify the most influential parameters for predicting the prevalence of malaria infection in the region. In particular, we performed a global sensitivity analysis based on Monte Carlo and FAST methods. This method estimates global sensitivity indices for each model parameter. The global sensitivity indices reflect the overall importance of each parameter in the prevalence of malaria infection.

4.3. Global sensitivity analysis on the compartments

First, since the knowledge of the model parameters is incomplete, we perform an uncertainty analysis of (± 1 days) on the compartments (λ_{fh}, λ_{fm}, λ_{vh}, λ_{vm}) by making all the parameters using the Latin hypercube sampling (LHS) (Marino et al., 2008; Massard et al., 2022). Then, we will perform a sensitivity analysis of the parameters (λ_{fh}, λ_{fm}, λ_{vh}, λ_{vm}) on the evolution of the compartments I_{fh}, I_{fm}, I_{vh} and I_{vm} in order to identify the most influential parameter using the Monte Carlo technique.

Fig. 10 show the variation in the number of humans and mosquitoes infected with falciparum (Figure a and b) and vivax (Figure c and d) when we vary the four transmission parameters (λ_{fh}, λ_{fm}, λ_{vh}, λ_{vm}) of the full model (1). The black curves show the time evolution I_{fh} and I_{fm}, while the dark blue and light blue regions show the interval between the quantiles $q05 - q95$ and $q25 - q75$ respectively. It can be seen that I_{fh} and I_{fm} are very sensitive to day changes. For example, in Fig. 10 (a and b), at day $t = 15$, a variation of one day leads to a number of infected humans from 10 to 150 and at day $t = 20$ to a number of infected mosquitoes from 100 to 2500 by facilparum. In Fig. 10 (c and d), the peak of the median is at day $t = 10$ for 28 of vivax infected humans as opposed to 18 for the black curve which is an increase of 10 of infected individuals. The peak of the median

Table 3
Parameter estimation for the vivax model.

Parameter	Value	Reference
τ_h	0.05/day	Mukandavire et al. (2009b)
d_h	0.97202/day	Estimated
τ_m	1000/day	Mushayabasa et al. (2014)
μ_{vh}	0.015145/day	Estimated
μ_h	0.00004/day	Jones et al. (2015)
λ_{vm}	0.6137/day	Estimated
μ_m	0.1429/day	Mukandavire et al. (2009b)
λ_{vh}	1.95054/day	Estimated
b	0.25/day	Mukandavire et al. (2009b)
α_{vh}	0.4123/day	Estimated

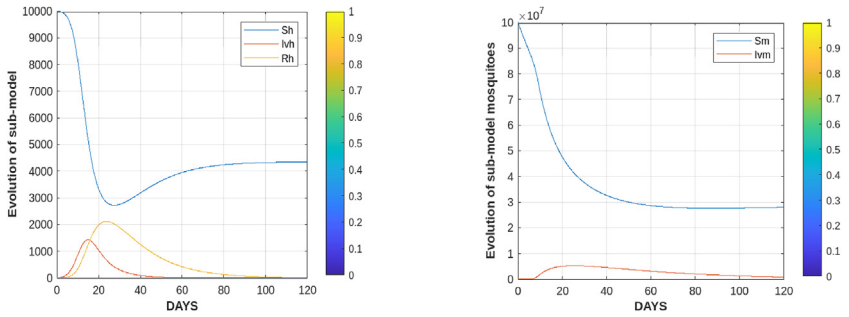

Fig. 7. Evolution humans and mosquitoes of sub-model Vivax with the estimated parameters $\lambda_{vh} = 1.95054$, $\alpha_{vh} = 0.4123$, $\lambda_{vm} = 0.6137$ and $\mathcal{R}_{0_v} = 2.6185$.

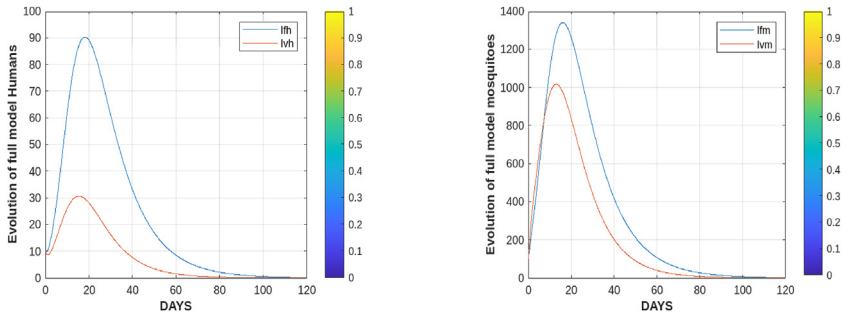

Fig. 8. Evolution of the human-mosquito infection for the full model.

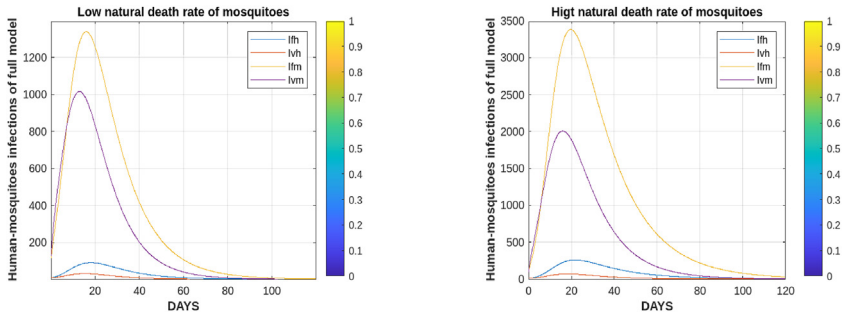

Fig. 9. Variations in human-mosquito infection as a function of mosquito mortality rates.

Table 4
Influence of the parameters on $\mathcal{R}_{0f}$.

Sensitivity Indices	λ_{fh}	λ_{fm}	α_{fh}	μ_{fh}	Sum of the indices	Time running
Monte Carlo	0.0301	0.2009	0.7605	0.0076	0.9991	2.216
FAST	0.0296	0.199	0.758	0.007	0.9936	0.333

Table 5
Influence of the parameters on $\mathcal{R}_{0v}$.

Sensitivity Indices	λ_{vh}	λ_{vm}	α_{vh}	μ_{vh}	Sum of indices	Time running
Monte Carlo	0.0304	0.3125	0.6494	0.0065	0.9988	2.0326
FAST	0.03057	0.3121	0.6483	0.0064	0.9973	1.6711

for vivax-infected mosquitoes is at day t = 15 for 500 of mosquitoes, versus 300 for the black curve, which is an increase of 200 of infected mosquitoes.

In Figs. 11–14, we have represented the singular influence of the parameters (λ_{fh}, λ_{fm}, λ_{vh}, λ_{vm}) on the compartments of human and mosquitoes infectants (I_{fh}, I_{fm}, I_{vh}, I_{vm}).

Figs. 11 and 12 show that the transmission parameters λ_{fh} and λ_{fm} act in the compartments of human infected (I_{fh}) and mosquitoes infected (I_{fm}) by Facilparum and do not act in the other two compartments infected by Vivax. We also note that the intensity of influence of λ_{fh} is much higher than the parameter λ_{fm} in both compartments (I_{fh} and I_{fm}). Conversely, in Figs. 13 and 14 the parameters λ_{vh} and λ_{vm} influence only the compartments infected by Vivax. We also note that the intensity of influence of λ_{vm} is much higher than the parameter λ_{vh} in both compartments (I_{vh} and I_{vm}).

This said, each of the parameters evolves according to the connected compartments, even if the influence is not the same: for example for t = 20 days the influence of λ_{fh} on I_{fh} reaches 200 infected persons while that of λ_{vh} on I_{vh} is 33 persons. And the influence of λ_{fm} on I_{fm} reaches 1900 infected mosquitoes while the influence of λ_{vm} on I_{vm} is 1350 number of mosquitoes.

5. Conclusion and discussion

In this study, we explore the dynamics of malaria infection in the Djibouti region using a mathematical model. Malaria infection is a phenomenon in which a person is infected with two or more different strains of parasites, which can have serious health consequences. In this study, we presented a mathematical model that takes into account the infections with different strains of parasites and the immunity acquired by individuals. We used statistical methods to fit the model to real data and analyze the dynamics of malaria infection. We calculated the basic reproduction rates of the sub-models (Falciparum and Vivax) and showed the existence, uniqueness and positivity of the solution of the system of equations. We showed the stability of the equilibrium points. A sensitivity analysis on the base reproduction rates ($\mathcal{R}_{0f}$ and $\mathcal{R}_{0v}$) of two sub-models (Falciparum and Vivax) has highlighted the most influential parameters. Next, we performed an uncertainty and sensitivity analysis on the infected compartments (human and mosquito). We found that each of the infection parameters acts on the compartment in which it is connected.

Biological significance. The analytical results of our study have epidemiological implications. Based on Djibouti data, we estimated that the basic reproductive number of Plasmodium Falciparum is higher than the basic reproductive number of Plasmodium vivax. Hence, we expect that for Djibouti, the Plasmodium falciparum might spread faster than Plasmodium vivax. The data in Figs. 3 and 6 is supporting this analytical result. This is an interesting biological observation, since a recent epidemiological review (Price et al., 2020) emphasized the fast spread of Plasmodium vivax in many geographical areas

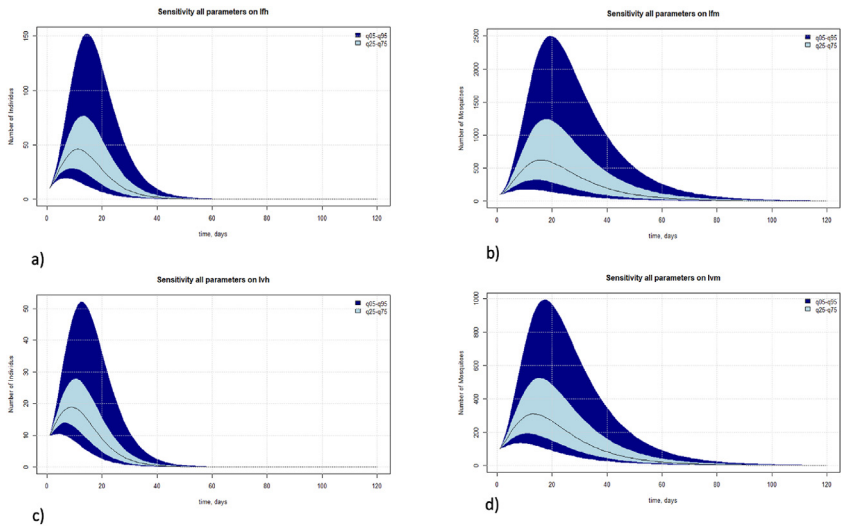

Fig. 10. Variability in the (a) I_{fh}, (b) I_{fm}, (c) I_{vh}, (d) I_{vm} output variables as we vary simultaneously, by a maximum of ±1 day, all transmission parameters that appear in the full model (1) (we vary these parameters according to the LHS scheme).

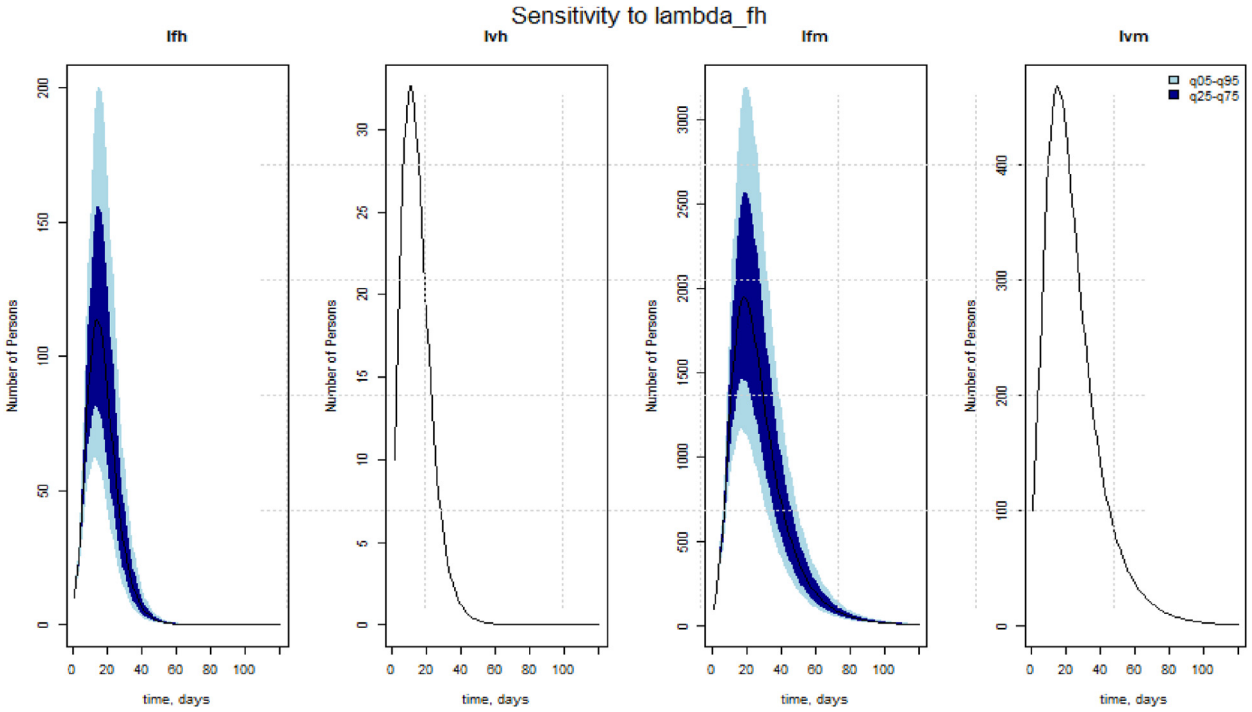

Fig. 11. Variability in the I_{fh}, I_{fm}, I_{vh} and I_{vm} output variables as we vary one single parameter, λ_{fh}, by ± 1 day.

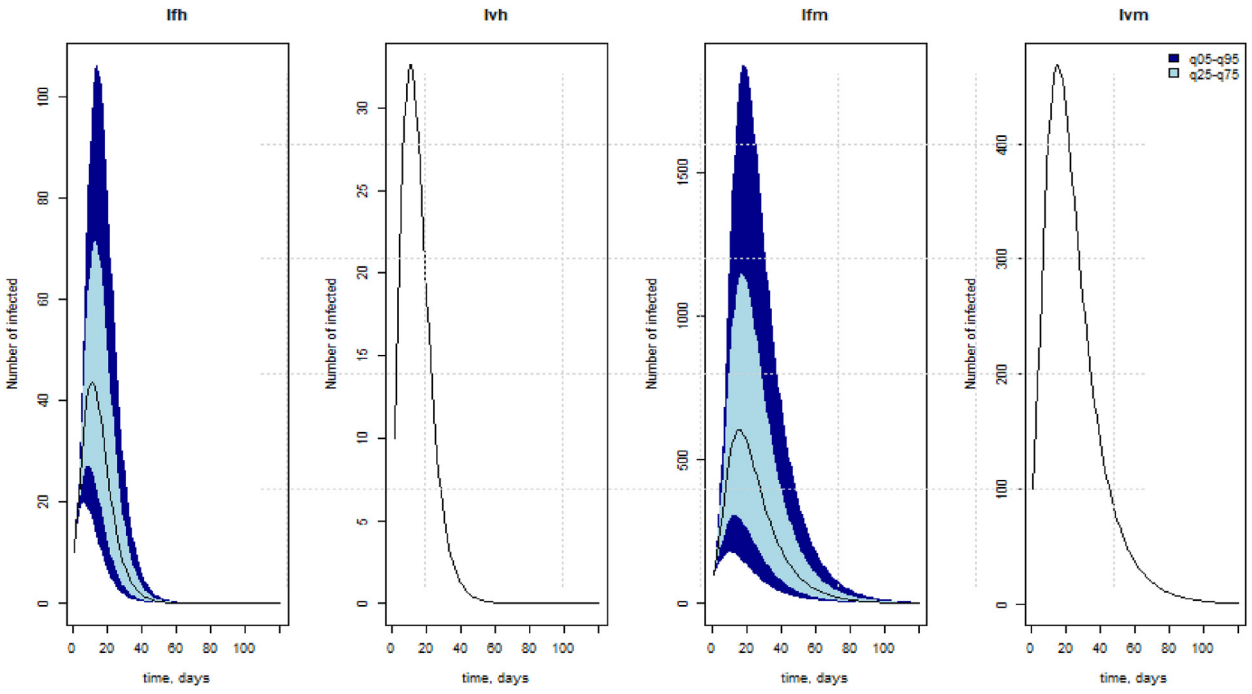

Fig. 12. Variability in the I_{fh}, I_{fm}, I_{vh} and I_{vm} output variables as we vary one single parameter, λ_{fm}, by ± 1 day.

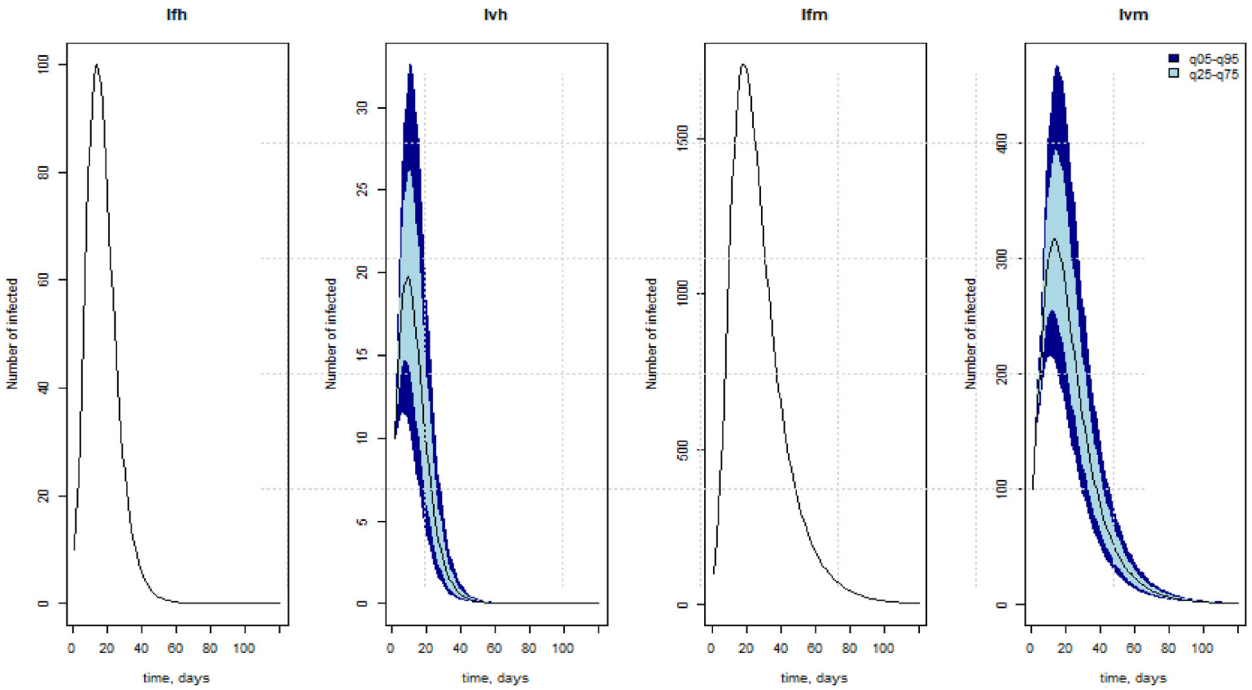

Fig. 13. Variability in the I_{fh}, I_{fm}, I_{vh} and I_{vm} output variables as we vary one single parameter, λ_{vh}, by ± 1 day.

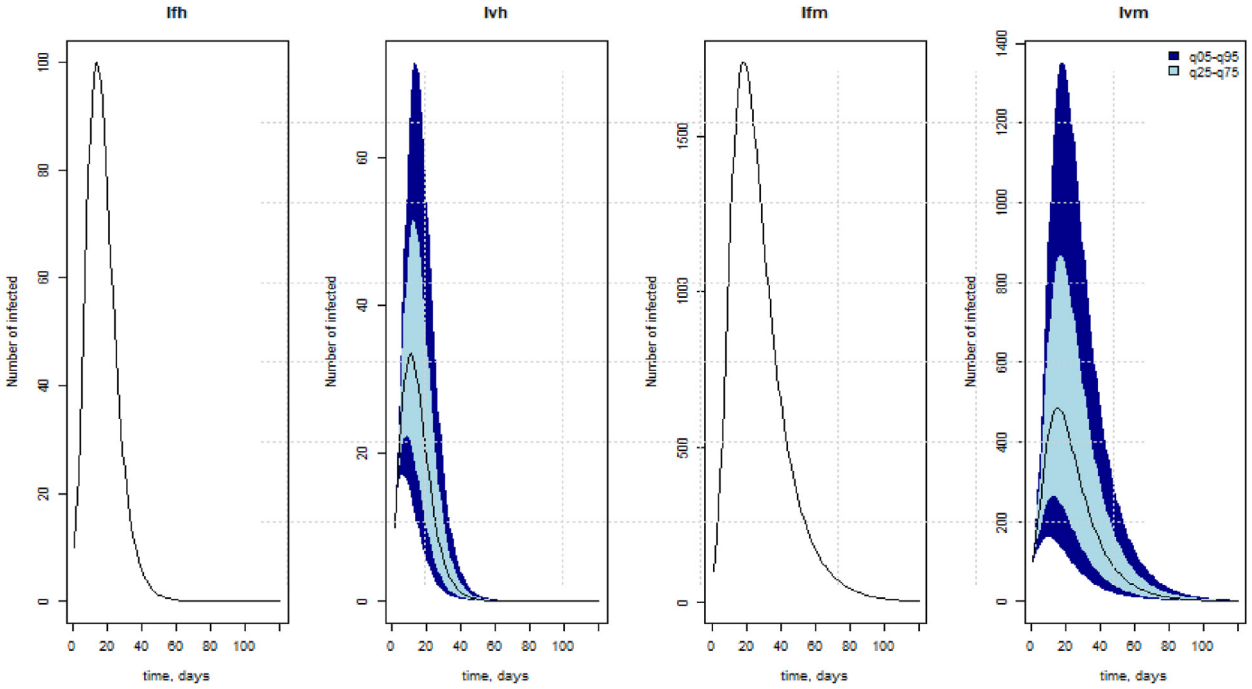

Fig. 14. Variability in the I_{fh}, I_{fm}, I_{vh} and I_{vm} output variables as we vary one single parameter, λ_{vm}, by ± 1 day.

(mainly outside of sub-Saharan Africa) where anti-malaria control activities have successfully reduced the incidence of Plasmodium falciparum (but these activities had less impact on reducing the transmission of P. Vivax). This suggests that even for Djibouti, the employment of anti-malaria control activities will eventually lead to a surge in P. Vivax, and new control activities will have to be employed at that time.

Comparison with published literature. A slightly different model that includes also exposed human and mosquito populations, as well as humans and mosquitoes co-infected with the two species at the same time, was developed in (Mahato et al., 2015) in the context of Indian data. Compared with the study in (Mahato et al., 2015) (that focused on the calculation of equilibrium points and of basic reproductive number, in addition to some numerical simulations), here we also carried out a global sensitivity analysis to investigate the impact of certain model parameters on the basic reproductive numbers and on the infected compartments. Moreover, we note that the different data sets corresponding to different geographical regions (Djibouti in this study vs. India in (Mahato et al., 2015)) led to different values for the basic reproductive ratios: here we obtained $\mathcal{R}_{0f} = 3.3692$ and $\mathcal{R}_{0v} = 2.6185$, while in (Mahato et al., 2015) the authors obtained $\mathcal{R}_{0f} = 1.3336$ and $\mathcal{R}_{0v} = 1.4151$. Therefore, while in India the P. Falciparum was less infectious than P. Vivax, in Djibouti we have seen the reversed scenario: P. Falciparum is more infectious than P. Vivax. In addition, the transmission of malaria in Djibouti seems to be much higher than the transmission in India. Overall, the results of this study emphasise the importance of investigating the malaria infections with different Plasmodium species across different geographical areas, as this could require different prevention and treatment strategies for all these different regions: Ali Sabieh, Dikhil, Tadjourah, Obock, Arta and Djibouti.

Other articles deal with the dynamics of Plasmodium vivax and Plasmodium falciparum reinfections. For example article (White et al., 2018), this article analyzes genotype samples from two longitudinal cohorts in Papua New Guinea and Thailand using a statistical model to estimate the acquisition and clearance times of each clone in each individual through a data augmentation process.

This study could be further extended to new mathematical models that incorporate different vaccination approaches, or incorporate different control approaches applied to the most influential parameters. It could also be extended to investigate the spatial spread of the two Plasmodium species (as different districts in Djibouti seem to be characterised by different numbers of P. Falciparum and P. Vivax cases (Moussa et al., 2023)), and the spatial competition between them. Finally, this work can be studied in the case of co-infections to see the interaction of this disease.

We note, for example, that a few other studies (Mason, 2000; Mason et al., 1999; Mason & Mckenzie, 1999; McQueen & McKenzie, 2006) focused on within-host mathematical models for the blood-stage dynamics of mixed Plasmodium vivax and Plasmodium falciparum infections in humans. The results in (Mason & Mckenzie, 1999) emphasized some characteristics observed in nature, namely that P. vivax infections can influence P. falciparum infections, notably by reducing their peak parasitemia. Moreover, the study in (Mason & Mckenzie, 1999) highlighted the possible complications when mixed infections were misdiagnosed and incorrectly treated. Therefore, even we could not find Djibouti data to support such mixed infections (which is consistent with older studies on the low prevalence of mixed-species infections (Cohen, 1973; Richie, 1988), we believe that the future incorporation of such an assumption into an extension of our model 1 could generate new testable biological hypotheses. Furthermore, the development of multi-scale models connecting between-host epidemiological infections and within-host blood infections, could help understand the impact of anti-malaria drugs that might not be as effective for all species in mixed infections.

Use of AI tools declaration

The authors declare they have not used Artificial Intelligence (AI) tools in the creation of this article.

Data availability

Data sets and numerical codes generated during the current study are available from the corresponding author on reasonable request.

CRediT authorship contribution statement

Yahyeh Souleiman: Writing – review & editing, Writing – original draft, Visualization, Validation, Supervision, Software, Resources, Project administration, Methodology, Investigation, Funding acquisition, Formal analysis, Data curation, Conceptualization. **Liban Ismail:** Writing – review & editing, Writing – original draft, Visualization, Methodology, Formal analysis, Data curation, Conceptualization. **Raluca Eftimie:** Validation, Supervision, Methodology, Conceptualization.

Declaration of competing interest

The authors declare that they have no known competing financial interests or personal relationships that could have appeared to influence the work reported in this paper.

Acknowledgments

This research work was funded by **CEALT** (Centre d'Excellence Africain en Logistique et Transport) of the University of Djibouti. The authors would like to thank **CEALT** for their financial support. R.E. acknowledges support from the MODCOV19 platform of the National Institute of Mathematical Sciences and their Interactions, **(CNRS)**.

The authors would like to thank the anonymous reviewers for their valuable remarks and constructive comments that contributed to improve the final version of the paper.

Appendix A. Proofs of positivity and bounding the solution theorems

Proof of Theorem 1. Taking into account the nonlinear system of equation (1), we consider the first equation

$$\frac{dS_h}{dt} = \tau_h + d_h R_h - (\mu_h\ N_h + \lambda_{fh}\ b\ I_{fm} + \lambda_{vh}\ b\ I_{vm})\frac{S_h}{N_h}, \tag{6}$$

which means that

$$\frac{dS_h}{dt} \geq -(\mu_h\ N_h + \lambda_{fh}\ b\ I_{fm} + \lambda_{vh}\ b\ I_{vm})\frac{S_h}{N_h}. \tag{7}$$

By using the exponential growth criterion and integrating (7) gives

$$S_h(t) \geqslant S_h(0) exp\left(-\int_0^t (\mu_h\ N_h(s) + \lambda_{fh}\ b\ I_{fm}(s) + \lambda_{vh}\ b\ I_{vm}(s))\frac{1}{N_h(s)} ds \right),$$

which implies $S_h(t) \geq 0$. By following similar steps as for the condition in $S_h(t)$, it can easily be shown that $S_m(t) \geq 0$, $I_{fh}(t) \geq 0$, $I_{vh}(t) \geq 0$, $I_{fm}(t) \geq 0$ and $I_{vm}(t) \geq 0$, $\forall t \geq 0$. □

Proof of Theorem 2. Adding the first eight equations, and the last two equations, of model (1) gives, respectively,

$$\frac{dN_h}{dt} = \tau_h - \mu_h N_h,$$
$$\frac{dN_m}{dt} = \tau_m - \mu_m N_m.$$

Since $\frac{dN_h}{dt} \leq \tau_h - \mu_h N_h$ and $\frac{dN_m}{dt} \leq \tau_m - \mu_m N_m$ it follows that $\frac{dN_h}{dt} \leq 0$ and $\frac{dN_m}{dt} \leq 0$ if $N_h(t) \geq \frac{\tau_h}{\mu_h}$ and $N_m(t) \geq \frac{\tau_m}{\mu_m}$, respectively. Hence, it follows, using comparison theorem (Lakshmikantham et al., 1989), that

$$N_h(t) \leq N_h(0)e^{-\mu_h} + \frac{\tau_h}{\mu_h}(1 - e^{-\mu_h}),$$
$$N_m(t) \leq N_m(0)e^{-\mu_m} + \frac{\tau_m}{\mu_m}(1 - e^{-\mu_m}).$$

In particular, $N_h(t) \leq \frac{\tau_h}{\mu_h}$ if $N_h(0) \leq \frac{\tau_h}{\mu_h}$ and $N_m(t) \leq \frac{\tau_m}{\mu_m}$ if $N_m(0) \leq \frac{\tau_m}{\mu_m}$, respectively. Thus, the region Ω is positively-invariant for the model (1). Furthermore, if $N_h(0) > \frac{\tau_h}{\mu_h}$ and $N_m(0) > \frac{\tau_m}{\mu_m}$, then either the solution enters Ω in finite time or, $N_h(t) \to \frac{\tau_h}{\mu_h}$ and $N_m(t) \to \frac{\tau_m}{\mu_m}$. Hence, the region Ω attracts all solutions in $\mathbb{R}^7$. □

Appendix B. Proofs of Theorem 3: Stability of the equilibrium states E_{0f} and The endemic equilibrium E_f^*

Let $\mathcal{F}_f$ represents the rate of new infection matrix and $\mathcal{V}_f$ denotes the transfer rate matrix of the individuals:

$$\mathcal{F}_f = \begin{pmatrix} \tau_h + d_h R_h \\ \frac{\lambda_{fh} b}{N_h} I_{fm} S_h \\ \tau_m \\ \frac{\lambda_{fm} b}{N_h} I_{fh} S_m \end{pmatrix}, \qquad \mathcal{V}_f = \begin{pmatrix} \left(\mu_h + \frac{\lambda_{fm} b}{N_h} I_{fm}\right) S_h \\ (\mu_h + \mu_{fh} + \alpha_{fh}) I_{fh} \\ \left(\mu_m + \frac{\lambda_{fm} b}{N_h} I_{fh}\right) S_m \\ \mu_m I_{fm} \end{pmatrix}.$$

Let us define

$$F_f = \frac{\partial \mathcal{F}_f}{\partial x_j}(E_{0f}) = \begin{pmatrix} 0 & 0 & 0 & 0 \\ 0 & 0 & 0 & \lambda_{fh} b \\ 0 & 0 & 0 & 0 \\ 0 & \frac{\lambda_{fm} b \tau_m \mu_h}{\tau_h \mu_m} & 0 & 0 \end{pmatrix},$$

and

$$V_f = \frac{\partial \mathcal{V}_f}{\partial x_j}(E_{0f}) = \begin{pmatrix} \mu_h & 0 & 0 & \lambda_{fh} b \\ 0 & (\mu_h + \mu_{fh} + \alpha_{fh}) & 0 & 0 \\ 0 & \frac{\lambda_{fm} b \tau_m \mu_h}{\tau_h \mu_m} & \mu_m & 0 \\ 0 & 0 & 0 & \mu_m \end{pmatrix}.$$

The reproduction number for the plasmodium falciprum model given by (2) can be calculated from the relation $\mathcal{R}_{0f}(t) = \rho(F_f V_f^{-1})$ with ρ the spectral radius of $F_f V_f^{-1}$, where

$$V_f^{-1} = \begin{pmatrix} \frac{1}{\mu_h} & 0 & 0 & -\frac{\lambda_{fh} b}{\mu_h \mu_m} \\ 0 & \frac{1}{\mu_h + \mu_{fh} + \alpha_{fh}} & 0 & 0 \\ 0 & -\frac{\lambda_{fm} b \tau_m \mu_h}{\tau_h \mu_m^2 \left(\mu_h + \mu_{fh} + \alpha_{fh}\right.} & \frac{1}{\mu_m} & 0 \\ 0 & 0 & 0 & \frac{1}{\mu_m} \end{pmatrix}.$$

and

$$F_f V_f^{-1} = \begin{pmatrix} 0 & 0 & 0 & 0 \\ 0 & 0 & 0 & \frac{\lambda_{fh} b}{\mu_m} \\ 0 & 0 & 0 & 0 \\ 0 & \frac{\lambda_{fm} b \tau_m \mu_h}{\tau_h \mu_m \left(\mu_h + \mu_{fh} + \alpha_{fh}\right.} & 0 & 0 \end{pmatrix}.$$

This number is found to be

$$\mathcal{R}_{0f} = \sqrt{\frac{\lambda_{fm} \lambda_{fh} b^2 \tau_m \mu_h}{\tau_h \mu_m^2 (\mu_h + \mu_{fh} + \alpha_{fh})}}.$$

Now, we shall establish the stability of the equilibrium states. The Jacobian matrix for any equilibrium point E_f of the model (2)

$$J(E_f) = \begin{pmatrix} -\left(\mu_h + \frac{\lambda_{fh} b I_{fm}}{N_h}\right) & 0 & d_h & 0 & -\frac{\lambda_{fh} b S_h}{N_h} \\ \frac{\lambda_{fh} b I_{fm}}{N_h} & -(\mu_h + \mu_{fh} + \alpha_{fh}) & 0 & 0 & \frac{\lambda_{fh} b S_h}{N_h} \\ 0 & \alpha_{fh} & -(\mu_h + d_h) & 0 & 0 \\ 0 & -\frac{\lambda_{fm} b S_m}{N_h} & 0 & -\left(\mu_m + \frac{\lambda_{fm} b I_{fh}}{N_h}\right) & 0 \\ 0 & \frac{\lambda_{fm} b S_m}{N_h} & 0 & \frac{\lambda_{fm} b I_{fh}}{N_h} & -\mu_m \end{pmatrix}.$$

The Jacobian matrix corresponding to the system (2) at DFE point $E_{0f} = \left(\frac{\tau_h}{\mu_h}, 0, 0, \frac{\tau_m}{\mu_m}, 0\right)$

$$J(E_{0f}) = \begin{pmatrix} -\mu_h & 0 & d_h & 0 & -\lambda_{fh} b \\ 0 & -(\mu_h + \mu_{fh} + \alpha_{fh}) & 0 & 0 & \lambda_{fh} b \\ 0 & \alpha_{fh} & -(\mu_h + d_h) & 0 & 0 \\ 0 & -\frac{\lambda_{fm} b \tau_m \mu_h}{\tau_h \mu_m} & 0 & -\mu_m & 0 \\ 0 & \frac{\lambda_{fm} b \tau_m \mu_h}{\tau_h \mu_m} & 0 & 0 & -\mu_m \end{pmatrix}.$$

The characteristic polynomial of the matrix J(E_{0f}) is

$$P(X) = (-\mu_h - X)(-\mu_m - X)(-\mu_h - d_h - X)\left(X^2 + k_{1f}X + k_{2f}\right),$$

where $k_{1f} = \left(\mu_m + \mu_h + \mu_{fh} + \alpha_{fh}\right)$ and $k_{2f} = \mu_m(\mu_h + \mu_{fh} + \alpha_{fh})\left(1 - \mathcal{R}_{0f}^2\right)$.

It can easily be seen that there are three obvious negative eigenvalues. For the other two eigenvalues, we will use the Routh-Hurwitz criterion (DeJesus & Kaufman, 1987) with $k_{1f} > 0$ and $k_{2f} > 0$ if $\mathcal{R}_{0f} < 1$. This concludes the disease free equilibrium is locally asymptotically stable if $\mathcal{R}_{0f} < 1$.

The endemic equilibrium $E_f^* = (S_h^*, I_{fh}^*, R_h^*, S_m^*, I_{fm}^*)$ are solutions of the system:

$$\frac{dS_h}{dt} = \frac{dI_{fh}}{dt} = \frac{dR_h}{dt} = \frac{dS_m}{dt} = \frac{dI_{fm}}{dt} = 0. \tag{8}$$

To begin with, we define β_{fh}^* and β_{fm}^* are the force of infections of humans and mosquitoes falciparum at the equilibrium point, given by

$$\beta_{fh}^* = \frac{\lambda_{fh}\, b}{N_h^*} I_{fm}^*, \qquad \beta_{fm}^* = \frac{\lambda_{fm}\, b}{N_h^*} I_{fh}^*. \tag{9}$$

From this system (8) and equation (9), we obtain:

$$\beta_{fh}^* S_h^* = (\mu_h + \mu_{fh} + \alpha_{fh}) I_{fh}^*, \quad R_h^* = \frac{\alpha_{fh}}{\mu_h + d_h} I_{fh}^*, \quad S_m^* = \frac{\tau_m}{\mu_m + \beta_{fm}^*} \quad \text{and} \quad I_{fm}^* = \frac{\tau_m\, \beta_{fm}^*}{\mu_m(\mu_m + \beta_{fm}^*)}.$$

Substituting I_{fm}^* into (9), we get:

$$\beta_{fh}^*\, N_h^*\, \mu_m(\mu_m + \beta_{fm}^*) - \lambda_{fh}\, b\, \tau_m\, \beta_{fm}^* = 0, \tag{10}$$

and, after long computations of system (2), we get

$$\beta_{fm}^* = \frac{c_{1f}\, \beta_{fh}^*}{c_{2f}\, \beta_{fh}^* + c_{3f}}, \tag{11}$$

where

$$c_{1f} = \tau_h\, b\, \lambda_{fm}(\mu_h + d_h)$$

and

$$c_{2f} = d_h\, N_h^*(\mu_h + \mu_{fm}) + \mu_h\, N_h^*(\mu_h + \mu_{fm} + \alpha_{fh})$$

and

$$c_{3f} = \mu_h\, N_h^*(\mu_h + d_h)(\mu_h + \mu_{fh} + \alpha_{fh}).$$

Now, substituting (10) into (11), we get

$$a_{0f}(\beta_{fh}^{*})^{2} + a_{1f}\beta_{fh}^{*} = 0, \tag{12}$$

where

$$a_{0f} = N_h^{*}\,\mu_m(\mu_m\, c_{2f} + c_{1f}), \quad \text{and} \quad a_{1f} = c_{3f}N_h^{*}\,\mu_m^{2}(1-\mathcal{R}_{0f}^{2}).$$

Note that a_{0f} is positive, and there is a unique endemic equilibrium if $a_{1f} < 0$ (i.e. if $\mathcal{R}_{0f} > 1$).

Appendix C. Proofs of Theorem 4: Stability of the equilibrium states E_{0v} and The endemic equilibrium E_v^{*}

Let $\mathcal{F}_v$ represents the rate of new infection matrix and $\mathcal{V}_v$ denotes the transfer rate matrix of the individuals:

$$\mathcal{F}_v = \begin{pmatrix} \tau_h + d_h R_h \\ \dfrac{\lambda_{fh} b}{N_h} I_{vm} S_h \\ \tau_m \\ \dfrac{\lambda_{vm} b}{N_h} I_{vh} S_m \end{pmatrix}, \qquad \mathcal{V}_v = \begin{pmatrix} \left(\mu_h + \dfrac{\lambda_{vm} b}{N_h} I_{vm}\right) S_h \\ (\mu_h + \mu_{vh} + \alpha_{vh}) I_{vh} \\ \left(\mu_m + \dfrac{\lambda_{vm} b}{N_h} I_{vh}\right) S_m \\ \mu_m I_{vm} \end{pmatrix}.$$

Let us define

$$F_v = \frac{\partial \mathcal{F}_v}{\partial x_j}(E_{0v}) = \begin{pmatrix} 0 & 0 & 0 & 0 \\ 0 & 0 & 0 & \lambda_{vh} b \\ 0 & 0 & 0 & 0 \\ 0 & \dfrac{\lambda_{vm} b \tau_m \mu_h}{\tau_h \mu_m} & 0 & 0 \end{pmatrix},$$

and

$$V_v = \frac{\partial \mathcal{V}_v}{\partial x_j}(E_{0v}) = \begin{pmatrix} \mu_h & 0 & 0 & \lambda_{vh} b \\ 0 & (\mu_h + \mu_{vh} + \alpha_{vh}) & 0 & 0 \\ 0 & \dfrac{\lambda_{vm} b \tau_m \mu_h}{\tau_h \mu_m} & \mu_m & 0 \\ 0 & 0 & 0 & \mu_m \end{pmatrix}.$$

The reproduction number for the plasmodium vivax model given by (4) can be calculated from the relation $\mathcal{R}_{0v}(t) = \rho(F_v V_v^{-1})$ with ρ the spectral radius of $F_v V_v^{-1}$, where

$$V_v^{-1} = \begin{pmatrix} \dfrac{1}{\mu_h} & 0 & 0 & -\dfrac{\lambda_{vh} b}{\mu_h \mu_m} \\ 0 & \dfrac{1}{\mu_h + \mu_{vh} + \alpha_{vh}} & 0 & 0 \\ 0 & -\dfrac{\lambda_{vm} b \tau_m \mu_h}{\tau_h \mu_m^{2} (\mu_h + \mu_{vh} + \alpha_{vh})} & \dfrac{1}{\mu_m} & 0 \\ 0 & 0 & 0 & \dfrac{1}{\mu_m} \end{pmatrix}.$$

and

$$F_v V_v^{-1} = \begin{pmatrix} 0 & 0 & 0 & 0 \\ 0 & 0 & 0 & \frac{\lambda_{vh} b}{\mu_m} \\ 0 & 0 & 0 & 0 \\ 0 & \frac{\lambda_{vm} b \tau_m \mu_h}{\tau_h \mu_m (\mu_h + \mu_{vh} + \alpha_{vh})} & 0 & 0 \end{pmatrix}.$$

This numbar is equal to

$$\mathcal{R}_{0v} = \sqrt{\frac{\lambda_{vm} \lambda_{vh} b^2 \tau_m \mu_h}{\tau_h \mu_m^2 (\mu_h + \mu_{vh} + \alpha_{vh})}}.$$

Now, we shall establish the stability of the equilibrium states. The Jacobian matrix for any equilibrium point E_v of the model (4)

$$J(E_v) = \begin{pmatrix} -\left(\mu_h + \frac{\lambda_{vh}\ b\ I_{vm}}{N_h}\right) & 0 & d_h & 0 & -\frac{\lambda_{vh}\ b\ S_h}{N_h} \\ \frac{\lambda_{vh}\ b\ I_{vm}}{N_h} & -(\mu_h + \mu_{vh} + \alpha_{vh}) & 0 & 0 & \frac{\lambda_{vh}\ b\ S_h}{N_h} \\ 0 & \alpha_{vh} & -(\mu_h + d_h) & 0 & 0 \\ 0 & -\frac{\lambda_{vm}\ b\ S_m}{N_h} & 0 & -\left(\mu_m + \frac{\lambda_{vm}\ b\ I_{vh}}{N_h}\right) & 0 \\ 0 & \frac{\lambda_{vm}\ b\ S_m}{N_h} & 0 & \frac{\lambda_{vm}\ b\ I_{vh}}{N_h} & -\mu_m \end{pmatrix}.$$

The Jacobian matrix corresponding to the system (4) at the DFE point $E_{0v} = \left(\frac{\tau_h}{\mu_h}, 0, 0, \frac{\tau_m}{\mu_m}, 0\right)$, is as follows

$$J(E_{0v}) = \begin{pmatrix} -\mu_h & 0 & d_h & 0 & -\lambda_{vh}\ b \\ 0 & -(\mu_h + \mu_{vh} + \alpha_{vh}) & 0 & 0 & \lambda_{vh}\ b \\ 0 & \alpha_{vh} & -(\mu_h + d_h) & 0 & 0 \\ 0 & -\frac{\lambda_{vm}\ b\ \tau_m \mu_h}{\tau_h \mu_m} & 0 & -\mu_m & 0 \\ 0 & \frac{\lambda_{fm}\ b\ \tau_m \mu_h}{\tau_h \mu_m} & 0 & 0 & -\mu_m \end{pmatrix}.$$

The characteristic polynomial of the matrix $J(E_{0v})$ is

$$P(X) = (-\mu_h - X)(-\mu_m - X)(-\mu_h - d_h - X)\left(X^2 + k_{1v}X + k_{2v}\right),$$

where $k_{1v} = (\mu_m + \mu_h + \mu_{vh} + \alpha_{vh})$ and $k_{2v} = \mu_m(\mu_h + \mu_{vh} + \alpha_{vh})\left(1 - \mathcal{R}_{0v}^2\right)$.

It can easily be seen that there are three obvious negative eigenvalues. For the other two eigenvalues, we will use the Routh-Hurwitz criterion (DeJesus & Kaufman, 1987) with $k_{1v} > 0$ and $k_{2v} > 0$ if $\mathcal{R}_{0v} < 1$. This concludes the disease free equilibrium is locally asymptotically stable if $\mathcal{R}_{0v} < 1$.

The endemic equilibrium $E_v^* = (S_h^*, I_{vh}^*, R_h^*, S_m^*, I_{vm}^*)$ are solutions of the system:

$$\frac{dS_h}{dt} = \frac{dI_{vh}}{dt} = \frac{dR_h}{dt} = \frac{dS_m}{dt} = \frac{dI_{vm}}{dt} = 0. \tag{13}$$

As in the previous case of falciparum, we also define β_{vh}^* and β_{vm}^* are the force of infections of humans and mosquitoes vivax at the equilibrium point, given by

$$\beta_{vh}^* = \frac{\lambda_{vh}\ b}{N_h^*} I_{vm}^*, \qquad \beta_{vm}^* = \frac{\lambda_{vm}\ b}{N_h^*} I_{vh}^*. \tag{14}$$

From this system (13) and equation (14) we obtain:

$$\beta^*_{vh} S^*_h = (\mu_h + \mu_{vh} + \alpha_{vh}) I^*_{fh}, \quad R^*_h = \frac{\alpha_{vh}}{\mu_h + d_h} I^*_{vh}, \quad S^*_m = \frac{\tau_m}{\mu_m + \beta^*_{vm}} \quad \text{and} \quad I^*_{vm} = \frac{\tau_m \ \beta^*_{vm}}{\mu_m(\mu_m + \beta^*_{vm})}.$$

Substituting I^*_{vm} into (14), we get:

$$\beta^*_{vh} \ N^*_h \ \mu_m(\mu_m + \beta^*_{vm}) - \lambda_{vh} \ b \ \tau_m \ \beta^*_{vm} = 0, \tag{15}$$

and, after long computations, we obtain

$$\beta^*_{vm} = \frac{c_{1v} \ \beta^*_{vh}}{c_{2v} \ \beta^*_{vh} + c_{3v}}, \tag{16}$$

where

$$c_{1v} = \tau_h \ b \ \lambda_{vm}(\mu_h + d_h)$$

and

$$c_{2v} = d_h \ N^*_h(\mu_h + \mu_{vm}) + \mu_h \ N^*_h(\mu_h + \mu_{vm} + \alpha_{vh})$$

and

$$c_{3v} = \mu_h \ N^*_h(\mu_h + d_h)(\mu_h + \mu_{vh} + \alpha_{vh}).$$

Now, substituting (15) into (16), we get

$$a_{0v}(\beta^*_{vh})^2 + a_{1v}\beta^*_{vh} = 0, \tag{17}$$

where

$$a_{0v} = N^*_h \ \mu_m(\mu_m \ c_{2v} + c_{1v}), \quad \text{and} \quad a_{1v} = c_{3v} N^*_h \ \mu^2_m(1 - \mathcal{R}^2_{0v}).$$

Note that a_{0v} is positive, and there is a unique endemic equilibrium if $a_{1v} < 0$ (i.e. if $\mathcal{R}_{0v} > 1$).

Appendix D. Proofs of Theorem 5: Stability of the equilibrium states E_0

The Jacobian matrix corresponding to the system (1) at the DFE point

$$E_0 = \left(\frac{\tau_h}{\mu_h}, 0, 0, 0, \frac{\tau_m}{\mu_m}, 0, 0\right),$$

is given by

$$J(E_0) = \begin{pmatrix} -\mu_h & 0 & 0 & d_h & 0 & -\lambda_{fh} \ b & -\lambda_{vh} \ b \\ 0 & -(\mu_h + \mu_{fh} + \alpha_{fh}) & 0 & 0 & 0 & \lambda_{fh} \ b & 0 \\ 0 & 0 & -(\mu_h + \mu_{vh} + \alpha_{vh}) & 0 & 0 & 0 & \lambda_{vh} \ b \\ 0 & \alpha_{fh} & \alpha_{vh} & -(\mu_h + d_h) & 0 & 0 & 0 \\ 0 & -\lambda_{fm} \ b & -\lambda_{vm} \ b & 0 & -\mu_m & 0 & 0 \\ 0 & \frac{\lambda_{fm} \ b \ \tau_m \ \mu_h}{\mu_m \ \tau_h} & 0 & 0 & 0 & -\mu_m & 0 \\ 0 & 0 & \frac{\lambda_{vm} \ b \ \tau_m \ \mu_h}{\mu_m \ \tau_h} & 0 & 0 & 0 & -\mu_m \end{pmatrix}.$$

The characteristic polynomial of the matrix $J(E_0)$ is

$$P(X) = (-\mu_h - X)(-\mu_m - X)(-\mu_h - d_h - X)\left(X^2 + k_{1f}X + k_{2f}\right)\left(X^2 + k_{1v}X + k_{2v}\right).$$

It can easily be seen that there are three obvious negative eigenvalues. For the other four eigenvalues, we will use the previous theorems 3 and 4 which give stability if $\mathcal{R}_{0f} < 1$ and $\mathcal{R}_{0v} < 1$ respectively. This concludes that the disease-free equilibrium is locally asymptotically stable if $\mathcal{R}_0 < 1$.

References

Agusto, F. B., & Tchuenche, J. M. (2013). Control strategies for the spread of malaria in humans with variable attractiveness. *Mathematical Population Studies, 20*(2), 82–100.
Cohen, J. E. (1973). Heterologous immunity in human malaria. *The Quarterly Review of Biology, 48*(3), 467–489.
Cukier, R. I., et al. (1973). Study of the sensitivity of coupled reaction systems to uncertainties in rate coefficients. I Theory. *The Journal of Chemical Physics, 59*(8), 3873–3878.
Cukier, R. I., Levine, H. B., & Shuler, K. E. (1978). Nonlinear sensitivity analysis of multiparameter model systems. *Journal of Computational Physics, 26*(1), 1–42.
Cukier, R. I., Schaibly, J. H., & Shuler, K. E. (1975). Study of the sensitivity of coupled reaction systems to uncertainties in rate coefficients. III. Analysis of the approximations. *The Journal of Chemical Physics, 63*(3), 1140–1149.
DeJesus, E. X., & Kaufman, C. (1987). Routh-Hurwitz criterion in the examination of eigenvalues of a system of nonlinear ordinary differential equations. *Physical Review A, 35*(12), 5288.
Deshkar, S. T., Tore, R. P., & Shrikhande, S. N. (2015). Concomitant triple infection of dengue, malaria and enteric fever–A rare case report. *IJHSR, 5*(7), 529–535.
Diekmann, O., Heesterbeek, J., & Roberts, M. G. (2010). "The construction of next-generation matrices for compartmental epidemic models". *Journal of The Royal Society Interface, 7*(47), 873–885.
Flores-Alanis, A., et al. (2017). Temporal genetic changes in Plasmodium vivax apical membrane antigen 1 over 19 years of transmission in southern Mexico. *Parasites & Vectors, 10*(1), 1–12.
Garrido-Cardenas, J. A., et al. (2019). Analysis of global research on malaria and Plasmodium vivax. *International Journal of Environmental Research and Public Health, 16*(11), 1928.
Hay, S. I., et al. (2005). Urbanization, malaria transmission and disease burden in Africa. *Nature Reviews Microbiology, 3*(1), 81–90.
Homma, T., & Saltelli, A. (1996). Importance measures in global sensitivity analysis of nonlinear models. *Reliab. Eng. Syst., 52.1*, 1–17.
Ismail, L., Djellout, H., & Chauvière, C. (2023). Climate system: A global sensitivity approach. *Iranian Journal of Science*, 1–17.
Jones, M. M., Wang, F.-B., & Vaidya, N. K. (2015). Modeling malaria and typhoid fever co-infection dynamics. *Mathematical Biosciences, 264*, 128–144.
Khaireh, B. A., et al. (2013). Population genetics analysis during the elimination process of Plasmodium falciparum in Djibouti. *Malaria Journal, 12*, 1–14.
Lakshmikantham, V., Leela, S., & Martynyuk, A. A. (1989). *Stability analysis of nonlinear systems*. Springer.
Long, E. F., Vaidya, N. K., & Brandeau, M. L. (2008). Controlling co-epidemics: Analysis of HIV and tuberculosis infection dynamics. *Operations Research, 56*(6), 1366–1381.
Loy, D. E., et al. (2017). Out of Africa: Origins and evolution of the human malaria parasites plasmodium falciparum and plasmodium vivax. *International Journal for Parasitology, 47*(2–3), 87–97.
M Sobol, I. (1993). Sensitivity analysis for non-linear mathematical models. *Math. Modeling Comput. Experiment, 1*, 407–414.
Mahato, B., et al. (2015). Mathematical model of malaria for Co-infection of plasmodium vivax and plasmodium falciparum in India. *British Microbiology Research Journal, 5*(3), 285.
Mandal, S., Sarkar, R. R., & Sinha, S. (2011). Mathematical models of malaria-a review. *Malaria Journal, 10*(1), 1–19.
Marino, S., et al. (2008). A methodology for performing global uncertainty and sensitivity analysis in systems biology. *Journal of Theoretical Biology, 254*(1), 178–196.
Mason, D. P. (2000). Review and recent progress: The mathematical modeling of mixed species plasmodium infections. *Southeast Asian Journal of Tropical Medicine & Public Health, 31*, 69–74.
Mason, D. P., & Mckenzie, F. E. (1999). Blood-stage dynamics and clinical implications of mixed Plasmodium vivax–Plasmodium falciparum infections. *The American Journal of Tropical Medicine and Hygiene, 61*(3), 367.
Mason, D. P., McKenzie, F. E., & Bossert, W. H. (1999). The blood-stage dynamics of mixed Plasmodium malariae–Plasmodium falciparum infections. *Journal of Theoretical Biology, 198*(4), 549–566.
Massard, M., et al. (2022). A multi-strain epidemic model for COVID-19 with infected and asymptomatic cases: Application to French data. *Journal of Theoretical Biology, 545*, 111–117.
McQueen, P. G., & McKenzie, F. E. (2006). Competition for red blood cells can enhance Plasmodium vivax parasitemia in mixed-species malaria infections. *The American Journal of Tropical Medicine and Hygiene, 75*(1), 112.
Mensah, J., Dontwi, J., & Bonyah, E. (2018). Stability analysis of zika-malaria coinfection model for malaria endemic region. *Journal of advances in Mathematics and computer science, 26*(1), 1–22.
Moussa, R. A., et al. (2023). Molecular investigation of malaria-infected patients in Djibouti city (2018–2021). *Malaria Journal, 22*(1), 147.
Mueller, I., et al. (2009). Key gaps in the knowledge of Plasmodium vivax, a neglected human malaria parasite. *The Lancet Infectious Diseases, 9*(9), 555–566.
Mukandavire, Z., et al. (2009a). Mathematical analysis of a model for HIV-malaria co-infection. *Mathematical Biosciences and Engineering, 6.2*, 333–362.
Mukandavire, Z., et al. (2009b). *Mathematical analysis of a model for HIV-malaria co-infection*.
Mushayabasa, S., Bhunu, C. P., & Mhlanga, N. A. (2014). Modeling the transmission dynamics of typhoid in malaria endemic settings. *Applications and Applied Mathematics: International Journal, 9*(1), 9.
Nnamonu, E. I., et al. (2020). Malaria: Trend of burden and impact of control strategies. *Int J Trop Dis Health, 41*, 18–30.
Ogunmiloro, O. M. (2019). Mathematical modeling of the coinfection dynamics of malaria-toxoplasmosis in the tropics. *Biometrical Letters, 56*(2), 139–163.
Okosun, K. O., & Makinde, O. D. (2014). A co-infection model of malaria and cholera diseases with optimal control. *Mathematical Biosciences, 258*, 19–32.
Olliaro, P. L., et al. (2016). Implications of Plasmodium vivax biology for control, elimination, and research. *The American Journal of Tropical Medicine and Hygiene, 95*(6 Suppl), 4.
Oluwafemi, T. J., Azuaba, E., & Kura, Y. M. (2020). Stablity analysis of disease free equilibrium of malaria, dengue and typhoid triple infection model. *Asian Research Journal of Mathematics, 16*, 11.
Porco, T. C., Small, P. M., Blower, S. M., et al. (2001). Amplification dynamics: Predicting the effect of HIV on tuberculosis outbreaks. *Journal of Acquired Immune Deficiency Syndromes, 28*(5), 437–444.
Price, R. N., et al. (2020). Plasmodium vivax in the era of the shrinking P. falciparum map. *Trends in Parasitology, 36.6*, 560–570.
Ray, M., Vazifdar, A., & Shivaprakash, S. (2020). Co-infection with malaria and coronavirus disease-2019. *Journal of Global Infectious Diseases, 12*, 3.
Richie, T. L. (1988). Interactions between malaria parasites infecting the same vertebrate host. *Parasitology, 96*(3), 607–639.
Rodriguez-Morales, A. J. (2008). Malaria: An eradicable threat? *The Journal of Infection in Developing Countries, 2*(1), 1–2.

Saltelli, A. (2002). Making best use of model evaluations to compute sensitivity indices. *Computer Physics Communications, 145.2*, 280–297.
Sankineni, S., et al. (2023). Global health and malaria: Past and present. In *Malarial drug delivery systems: Advances in treatment of infectious diseases* (pp. 1–16). Springer.
Sardar, S., et al. (2020). COVID-19 and Plasmodium vivax malaria co-infection. *IDCases, 21*.
Schaibly, J. H., & Shuler, K. E. (1973). Study of the sensitivity of coupled reaction systems to uncertainties in rate coefficients. II Applications. *Chemical Physics, 59*(8), 3879–3888.
Seidu, B., Makinde, O. D., & Seini, I. Y. (2015). Mathematical analysis of the effects of HIV-malaria co-infection on workplace productivity. *Acta Biotheoretica, 63*(2), 151–182.
Shah, N. H., & Gupta, J. (2014). HIV/AIDS-Malaria Co-infection dynamics. *Research Journal of Modeling and Simulation, 8*, 1–13.
Sobol, I. M. (2001). Global sensitivity indices for nonlinear mathematical models and their Monte Carlo estimates. *Mathematics and Computers in Simulation, 55*(1–3), 271–280.
Somma, S. A., et al. (2017). Stability analysis of disease free equilibrium (DFE) state of a mathematical model of yellow fever incorporating secondary host. *Pacific Journal of Science and Technology, 18*(2), 110–119.
Souleiman, Y., Mohamed, A., & Ismail, L. (2021). Analysis the dynamics of SIHR model: COVID-19 case in Djibouti. *Applied Mathematics, 12.10*, 867–881.
Suresh, V., et al. (2013). A rare case of triple infection with dengue, malaria and typhoid-A case report. *International Journal of Research & Development of Health, 1*(4), 200–203.
Tuju, J., et al. (2017). Vaccine candidate discovery for the next generation of malaria vaccines. *Immunology, 152*(2), 195–206.
White, M. T., et al. (2018). Plasmodium vivax and plasmodium falciparum infection dynamics: Re-infections, recrudescences and relapses. *Malaria Journal, 17*(1), 1–15.
Workie, Z. A., & Koya, P. R. (2022). Mathematical modelling of the Co-infection dynamics of typhoid fever with plasmodium vivax and plasmodium falciparum with treatment. *Mathematical Modelling and Applications, 7.1*, 1–25.
World Health Organization. (2022). *World malaria report 2022*. World Health Organization.